Clim. Past Discuss., https://doi.org/10.5194/cp-2018-100
Manuscript under review for journal Clim. Past
Discussion started: 27 August 2018

Climate of the Past Discussions

Speleothem Evidence for Megadroughts in the SW Indian Ocean during the Late Holocene

Hanying Li[1], Hai Cheng[1, 2*], Ashish Sinha[3], Gayatri Kathayat[1], Christoph Spötl[4], Aurèle Anquetil André[5], Arnaud Meunier[5], Jayant Biswas[6], Pengzhen Duan[1], Youfeng Ning[1], R. Lawrence Edwards[2]

[1] Institute of Global Environmental Change, Xi'an Jiaotong University, China
[2] Department of Earth Sciences, University of Minnesota, Minneapolis, USA
[3] Department of Earth Science, California State University Dominguez Hills, Carson, USA
[4] Department of Earth and Environmental Sciences, University of Illinois, Chicago, USA
[5] Francois Leguat Giant Tortoise and Cave Reserve, Anse Quitor, Rodrigues Island, Mauritius.
[6] National Cave Research and Protection Organization, Raipur, 492001, India.

*Correspondence and requests for materials should be addressed to H.C. (email: cheng021@xjtu.edu.cn)

Abstract

The '4.2 ka BP event' is widely described as a 200-300 years long interval of major climate anomaly (typically, arid and cooler conditions potentially across the globe), which defines the beginning of the current 'Meghalayan' age in the Holocene epoch. The 4.2 ka event however, has been disproportionately reported from proxy records situated at low-mid latitudes in the Northern Hemisphere. Consequently, the climatic manifestation of the 4.2 ka event in both spatial and temporal domains is still much less clear in Southern Hemisphere. This is particularly the case for the southwest sector of the southern Indian Ocean. Here we present high-resolution and chronologically well-constrained speleothem oxygen and carbon isotopes records of hydroclimate variability between ~6 and 3 ka ago from Rodrigues Island, located in the southwest subtropical Indian Ocean, ~ 600 km east of Mauritius. Our records reveal a major shift to drier condition at circa 4 ka BP, which culminated into a multicentennial period of drought (i.e., megadrought) that lasted continuously from ~ 3.9 to 3.5 ka BP. The inferred hydroclimatic conditions between 4.0 and 4.2 ka BP, are however not distinctly distinguishable from the region's mean hydroclimatic state over the length of our record. Because the precipitation variability at Rodrigues is distinctly modulated by meridional movement of the Inter-Tropical Convergence Zone and the El Niño Southern Oscillation dynamics, our proxy data may ultimately provide critical constraints in our understanding the timing and dynamical forcing of the 4.2 ka event.

Clim. Past Discuss., https://doi.org/10.5194/cp-2018-100
Manuscript under review for journal Clim. Past
Discussion started: 27 August 2018

1. Introduction

The '4.2 ka event' is a widespread climate event that occurred between ~ 4.2 and 3.9 ka BP (thousand years before present, where present =1950 AD) (e.g., Weiss et al., 2016). Many paleoclimate records from Northern Hemisphere (NH) have characterized the event as a multidecadal-multicentennial period of arid and cooler conditions across the Mediterranean, the Middle East, South Asia and North Africa (e.g., Finné et al., 2011; Marchant and Hooghiemstra, 2004; Migowski et al., 2006; Mayewski et al., 2004; Staubwasser et al., 2003; Arz et al., 2006; Zielhofer et al., 2017; Stanley et al., 2003; Kathayat et al., 2017). While some Southern Hemisphere (SH) proxy records from the tropical and sub-tropical regions of Africa and South America also show a shift to a drier climatic regime around 4 ka BP (e.g., Thompson et al., 2002; Russell et al., 2003; Marchant & Hooghiemstra, 2004), many other proxy records also show spatially complex and heterogeneous climate patterns around this time (e.g., Mayewski et al., 2004; Wanner et al., 2008; Russell et al., 2003; Berke et al., 2012; Tierney et al., 2011; Verschuren et al., 2009; de Boer et al., 2013, 2014, 2015; Rijsdijk et al., 2009, 2011; Tierney et al., 2008).

The driving mechanisms of the 4.2 ka event also remain elusive. For example, there is no clear evidence of rapid freshwater injection in the north Atlantic that could have disrupted the thermohaline circulation, and thereby, produced attendant changes in global climate in a manner akin to the 8.2 ka BP event (e.g., Walker et al., 2012). There are also no evidences of major perturbations in atmospheric concentrations of aerosols and CO_2 around this time (Monnin et al., 2001). A southward meridional shift in the mean position of the Inter-Tropical Convergence Zone (ITCZ) during this time has also been hypothesized (Mayewski et al., 2004), which potentially can account for the low–latitude aridity in many NH locations but this hypothesis is inconsistent with results from some proxy records situated at the southern margin of the ITCZ in SH, which show little or no evidence of wetter condition during this time (e.g., Russell et al., 2003; de Boer et al., 2013, 2014, 2015; Rijsdijk et al., 2009, 2011; Berke et al., 2012). Another hypothesis calls for a switch-on of the modern El Niño Southern Oscillation (ENSO) regime (e.g., Donders et al., 2008; Conroy et al., 2008), which became more pronounced in the mid-latitude regions after ca. 4 ka BP (e.g., Barron and Anderson, 2010). Although a marked asymmetrical increase in the ENSO variance (i.e., more frequent El Niño events) can account for the weakened Asian monsoon during the 4.2 ka BP event, but what impacts it may have had on the mid-latitudes climates in both hemisphere is not clear.

Here we present two precisely dated speleothem oxygen ($\delta^{18}O$) and carbon ($\delta^{13}C$) isotope records from La Vierge cave (LAVI-4) and Patate cave (PATA-1) from Rodrigues Island (Fig.1), located in the southern subtropical Indian Ocean. The LAVI-4 and PATA-1 records span from 6.0 to 3.0 ka BP and 6.1 to 3.5 ka BP, with average resolutions of ~4 and ~14 years, respectively. Our new records have tight

Clim. Past Discuss., https://doi.org/10.5194/cp-2018-100
Manuscript under review for journal Clim. Past
Discussion started: 27 August 2018

age control and sub-decadal resolution, which allow us to characterize hydroclimate variations in the southwestern Indian Ocean between 3 and 6 ka BP interval.

2 Cave Location and Modern Climatology

2.1 Climatology

Rodrigues (~19°42'S, ~63°24'E) is a small volcanic island (~120 km^2) situated in the southwestern Indian Ocean, ~600 km east of Mauritius (Fig. 1). The island's maximum altitude is ~400 m above sea level. Rodrigues' mean annual temperature is ~24°C and the mean annual rainfall is ~1010 mm, of which nearly 70% occurs during the wet season (November to April) with February being the wettest month. The seasonal distribution of rainfall is largely controlled by the seasonal migration of the ITCZ and the Mascarene High (Senapathi et al., 2010; Rijsdijk et al., 2011; Morioka et al., 2015) (Fig. 1). Given its location at the southern fringe of the ITCZ, the austral summer rainfall at Rodrigues is sensitive to the mean position of the southern limit of the ITCZ. This is highlighted by backward (~120 hours) HYSPLIT (Draxler and Hess, 1998) trajectory composites of the low level winds (850 hPa) for years when the total January to March (JFM) precipitation was unusally low (dry) and high (wet) than the long-term mean (1951-2016) at Rodrigues (Fig. 1B). Of note is a major increase in fraction of air parcel trajectories arriving from the north of Rodrigues during the wetter years, indicating an enhanced contribution of northerly moisture resulting from a more southern position of the ITCZ (Fig. 1B). This observation is further supported by low level wind trajectory clusters composites for the month of February for those years when the southern boundary of the the ITCZ was anomolusly north or south (Lashkari et al., 2017; Freitas et al., 2017) of its long-term mean February position (Fig. 2 A-B). In addition to the ITCZ, the ENSO dynamics also modulate austral summer precipiation in Rodrigues via modulating the Hadley and Walker circulations. (Senapathi et al., 2010; de Boer et al., 2014; Griffiths et al., 2016; Zinke et al., 2016). Instrumental data and our trajectory composites for select El Niño and La Niña years suggest that an increased (decreased) summer precipitation at Rodrigues are associated with the El Niño (La Niña) events (Fig. 2 C-D).

2.2 Oxygen isotope climatology

The modern observations of $\delta^{18}O$ of precipitation ($\delta^{18}O_p$) in the study area are unavailable due to lack of Global Network of Isotopes in Precipitation (GNIP) stations in Rodrigues. However, $\delta^{18}O_p$ data from the nearest GNIP station in Mauritius show a clear annual cycle in $\delta^{18}O_p$ with depleted values during the austral summer (Fig. 3A). Additionally, in absence of GNIP data, we use simulated $\delta^{18}O_p$ data from the Experimental Climate Prediction Center's Isotope-incorporated Global Spectral Model (IsoGSM) (Yoshimura et al., 2008) to assess the large-scale dynamical processes that control $\delta^{18}O_p$ on interannual and decadal timescales. Model results show the presence of a strong negative correlation between the $\delta^{18}O_p$ and rainfall amount similar to the 'amount effect' (e.g., Dansgaard, 1964) (Fig. 3 B-

Clim. Past Discuss., https://doi.org/10.5194/cp-2018-100
Manuscript under review for journal Clim. Past
Discussion started: 27 August 2018

C). We therefore, interpret $\delta^{18}O_p$ variations in the cave catchment and consequently, in speleothems from this region to primarily reflect variations in the rainfall amount in response to both local and large-scale atmospheric circulation changes in such that more negative (positive) $\delta^{18}O_p$ values occur during times of anomalous southward (northward) position of the southern boundary of the ITCZ and the El Niño (La Niña) conditions, respectively.

3 Methods and Results

3.1 Speleothem Samples

Two stalagmite samples, LAVI-4 and PATA-1, from La Vierge cave and Patate cave respectively, are used in this study. La Vierge (19°45′26″S, 63°22′13″E, ~32 masl) and Patate (19°45′30″S, 63°23′11″E, ~20 masl) caves are located in Plaine Corail and Plaine Caverne in southwestern Rodrigues, respectively (Middleton and Burney, 2013). The cave temperature and relative humidity at the time of sample collection (June 2015) were ~25.5°C and 95% in La Vierge cave and ~22.5°C and 95% in Patate cave, respectively. Samples LAVI-4 and PATA-1 were collected at the distance of ~50 m and 200 m from cave entrances, respectively. The diameters of LAVI-4 and PATA-1 are ~75 and 95 mm, and the length ~400 and ~334 mm, respectively. Both stalagmite samples were cut along their growth axes, using a thin diamond blade, and then polished. Both samples grew continuously between 3.5 and 6.0 ka BP interval without any visible hiatuses (Fig. 4).

3.2 ^{230}Th Dating

Subsamples (~80-130 mg) for ^{230}Th dating from LAVI-4 and PATA-1 were drilled using a 0.9 mm carbide dental drill. The ^{230}Th dating was performed at Xi'an Jiaotong University, China by using Thermo-Finnigan Neptune-*plus* multi-collector inductively coupled plasma mass spectrometers (MC-ICP-MS). The methods were described in Cheng et al. (2000, 2013). We used standard chemistry procedures (Edwards et al., 1987) to separate U and Th. A triple-spike (^{229}Th–^{233}U–^{236}U) isotope dilution method was used to correct instrumental fractionation and to determine U/Th isotopic ratios and concentrations (Cheng et al., 2000, 2013). U and Th isotopes were measured on a MasCom multiplier behind the retarding potential quadrupole in the peak-jumping mode using the standard procedures (Cheng et al., 2000). Uncertainties in U and Th isotopic measurements were calculated offline at 2σ level, including corrections for blanks, multiplier dark noise, abundance sensitivity, and contents of the same nuclides in spike solution. ^{234}U and ^{230}Th decay constants are reported in Cheng et al. (2013). Corrected ^{230}Th ages assume the initial ^{230}Th/^{232}Th atomic ratio of $4.4 \pm 2.2 \times 10^{-6}$, the values for material at secular equilibrium with the bulk earth ^{232}Th/^{238}U value of 3.8. The corrections for a few dating results of sample LAVI-4 and PATA-1 are large because either the U concentrations are relatively low (~65 ppb) or the detrital ^{232}Th concentrations are relatively high (>100 ppt) (Table S1, Fig. 5).

Clim. Past Discuss., https://doi.org/10.5194/cp-2018-100
Manuscript under review for journal Clim. Past
Discussion started: 27 August 2018

3.3 Age Models

We obtained 26 and 5 ^{230}Th dates for samples LAVI-4 and PATA-1, respectively. The LAVI-4 and PATA-1 age models and associated uncertainties were constructed using COPRA (Constructing Proxy Records from Age) (Breitenbach et al., 2012) and ISCAM (Fohlmeister, 2012) age modelling schemes (Fig. 4). Both modelling schemes yielded virtually identical age models, and thus conclusions of this study are not sensitive to the choice of different age models (Figs. 4 and 5).

3.4 Stable Isotope Analysis

LAVI-4 and PATA-1 stable isotope ($\delta^{18}O$ and $\delta^{13}C$) records are established by ~952 and ~192 data, respectively. The New Wave Micromill, a digitally controlled tri-axial micromill equipment, was used to obtain subsamples. The subsamples (~80 μg) were continuously micromilled from LAVI-4 and PATA-1 with typical increments between of 200 and 100 μm along the stalagmites growth axes, respectively. The subsamples of LAVI-4 were measured using Finnigan MAT-253 mass spectrometer coupled with an on-line carbonate preparation system (Kiel-IV) in the Isotope Laboratory, Xi'an Jiaotong University. The subsample of PATA-1 were measured using an on-line carbonate preparation system (GasbenchII) connected to an isotope ratio mass spectrometer (Delta^{plus}XL) in the Isotope Laboratory, Innsbruck University. The technique used in the Innsbruck University are reported in Spötl (2011) and Spötl and Vennemann (2003). All results are reported in per mil (‰) relative to the Vienna PeeDee Belemnite (VPDB) standard. Duplicate measurements of standards show a long-term reproducibility of ~0.1‰ (1σ) or better (Table S2, Fig. 5).

3.5 Isotopic Equilibrium Test

Conventional criteria for stalagmite isotopic equilibrium assessment is the Hendy Test (Hendy, 1971), which require weak or no correlation between speleothem $\delta^{18}O$ and $\delta^{13}C$ values measured along the growth axis as well as along the same growth lamina. The correlation between the $\delta^{18}O$ and $\delta^{13}C$ values in LAVI-4 and PATA-1 are 0.53 and 0.85, respectively, which on the basis of the Hendy Test, may indicate disequilibrium. However, some studies (e.g. Dorale and Liu, 2009) suggest that weak correlation between $\delta^{18}O$ and $\delta^{13}C$ values is not a prerequisite to isotopic equilibrium. Instead, the replication test (i.e., a high degree of coherence between individual $\delta^{18}O$ profiles of different speleothems from the same cave over the period of overlap) is a more stringent and reliable test of isotopic equilibrium. Indeed, a high degree of visual similarity between the coeval portions of LAVI-4 and PATA-1 $\delta^{18}O$ and $\delta^{13}C$ records suggest that both the stalagmites record primary climate signal, notwithstanding the offsets between the absolute values in two records (Fig. 5A). This is also confirmed by statistically significant correlations between the LAVI-4 and PATA-1 $\delta^{18}O$ ($r = 0.61$ at 95% confidence level) and $\delta^{13}C$ ($r = 0.69$ at 95% confidence level) records obtained through the ISCAM (Intra-Site Correlation Age Modelling) algorithm (Fohlmeister, 2012) during their contemporary growth

Clim. Past Discuss., https://doi.org/10.5194/cp-2018-100
Manuscript under review for journal Clim. Past
Discussion started: 27 August 2018

period between ~3.4–6.0 ka BP (Fig. 5). ISCAM strives to find the best correlation between the proxy records by adjusting each record within the margin of dating uncertainty by using a Monte Carlo approach. The significant levels are assessed against a red-noise background from generating artificially simulated first-order autoregressive time series (AR1). The offset in absolute $\delta^{18}O$ values between the LAVI-4 and PATA1 however, remains unclear, possibly arising from processes related to different karstic characteristics of the two caves. Therefore, in the following discussion we focus only the LAVI-4 $\delta^{18}O$ and $\delta^{13}C$ records due to their higher resolution, robust chronology and high-fidelity.

4 Discussion and Conclusions

4.1 Proxy Interpretations

The temporal resolution of LAVI-4 $\delta^{18}O$ profile between 3 and 6 ka BP varies from 1.2 to 16.4 years with an average resolution of ~3.2 years and is characterized by a large (~4.0 ‰) variability. As noted earlier, we interpret temporal variations in the LAVI-4 profile to dominantly reflect changes in the precipitation amount. This line of reasoning is justified given the island's isolated setting far removed from large-sized landmasses and its low topographic relief, which minimizes isotopic variability stemming from processes such as the continentality and altitude effects as well as mixing of distant water vapor sources with significantly different isotopic compositions. This interpretation is additionally supported by moderate to strong covariance between the LAVI-4 $\delta^{18}O$ and $\delta^{13}C$ profiles. Although the temporal variations in the latter can stem from changes in vegetation type and density, soil microbial productivity, prior calcite precipitation (PCP) and ground water infiltration rates (e.g., Baker et al., 1997; Genty et al., 2003), all of which may drive $\delta^{18}O$ and $\delta^{13}C$ values in the same fashion (e.g., Brook et al., 1990; Dorale et al., 1992; Bar-Matthews and Ayalon, 1997). The significant covariance between $\delta^{13}C$ and $\delta^{18}O$ records could therefore, indicate that both proxies reflect a common response to changes in rainfall amount at Rodrigues.

4.2 Hydroclimate Variability between 6 and 3 ka BP at Rodrigues

The LAVI-4 $\delta^{18}O$ and $\delta^{13}C$ records from 6 to 3 ka BP show prominent multidecadal to multicentennial scale variability but no clear long-term trends (Fig. 5 and 6). The z-score transformed profile of LAVI-4 $\delta^{18}O$ profile reveals several decadal to multidecadal intervals of significantly drier and wetter conditions (> ±1 standard deviation) (Fig. 6) that occurred throughout the length of the record. One of the most prominent features of our record is a switch from an interval characterized by $\delta^{18}O$ high-frequent variance (i.e., 6 to 4 ka BP) to the one with progressively higher $\delta^{18}O$ values from ~4 to 3.55 ka BP, suggesting a prolonged multi-centennial megadrought occurred in Rodrigues. After 3.54 ka BP, the $\delta^{18}O$ sharply decreased again until 3.12 ka BP, indicating the abrupt end of the megadrought (Fig. 6). The LAVI-4 $\delta^{13}C$ record shows a variation pattern broadly similar with the $\delta^{18}O$ record and delineates three major drought events between 6 and 3 ka, centered at 5.43, 4.62 and 3.54 ka

Clim. Past Discuss., https://doi.org/10.5194/cp-2018-100
Manuscript under review for journal Clim. Past
Discussion started: 27 August 2018

BP respectively, ~ 800-1000 years apart. All the three drought events show a saw-tooth pattern characterized by a long-term gradual positive excursion followed by an abrupt termination (Fig. 6). The interval corresponding to the '4.2 ka event', typically considered between 4.2 and 3.9 ka BP (e.g., Weiss et al., 2016), in the LAVI-4 records does not however, stand out as 'pulse-like' event as evident in many other proxy records. Instead, as noted above, it marks the onset of a multicentennial trend towards drier condition near the end of the typical '4.2 ka event' interval.

4.3 Broader Spatial Patterns of Hydroclimate Variability between 6 and 3 ka BP

The most prominent interval of drier hydroclimatic condition in our record between 3.9 and 3.5 is also evident in other records from Southeast Africa, such as records from Lake Edward (Russell et al., 2003), Lake Victoria (Berke et al., 2012), Zambezi delta (Schefuß et al., 2011) and Tatos basin (de Boer et al., 2014) (Fig. 7). Additionally, the record from Lake Malawi, East Africa (Konecky et al., 2011) also shows a weak dry excursion between 4.1 to 3.5 ka BP in the context of continuously wet trend between 6 and 3 ka BP. In the eastern sector of the southern Indian Ocean, speleothem records from Sumatra, Indonesia (Wurtzel et al., 2018), Northwest Australia (Denniston et al., 2013), and Liang Luar cave (Griffiths et al., 2009) also show the onset of generally drier conditions from ~ 4 ka BP (Fig. 8).

Previously, multiple hypotheses have been proposed to explain the onset of drier conditions ~ 4 ka BP in the southwestern Indian Ocean and Southeast Africa, which include shifts in the mean position of the ITCZ (Russell et al., 2005; Railsback et al., 2018), changes in the sea surface temperature (SST) gradient between western and eastern Indian Ocean (Indian Ocean Dipole, IOD) (Berke et al., 2012; de Boer et al., 2014), and increase in the ENSO variance (Tierney et al., 2011; de Boer et al., 2014). If IOD or ENSO is the main driving mechanism, an anti-phased relation between the Rodrigues record in the west and proxy record from eastern margin of the southern Indian Ocean including northern Australia would be expected (e.g., see the spatial pattern of El Niño related precipitation anomalies in Fig. 2D), which is inconsistent with phase relationship presented in the Fig. 8. As such therefore, IOD and ENSO does not readily explain the observed relationships between Rodrigues and other sites across the southern Indian Ocean.

A progressive trend towards drier condition in Rodrigues between ~4 and 3.5 ka BP suggest a northward shift in the mean position of the ITCZ (e.g., Fig. 2A). This inference, if correct, stands in direct contrast with the postulated southward shift in the ITCZ, often invoked to explain the weakening of the Asian monsoons since ~ 4.2 ka BP (e.g., Kathayat et al., 2017; Wang et al., 2005). Consequently, drier conditions on both northern and southern margins of the ITCZ in both hemispheres, argue against the idea of a simple southward shift in the mean position of the ITCZ as a probable cause of the 4.2 ka event. A more probable mechanism may therefore involve an overall contraction in the north-south range of the migrating ITCZ belt (e.g., Yan et al., 2015; Denniston et al., 2016; Scroxton et al., 2017) together with its reduced width which appears to better explain the spatial pattern of hydroclimate

change observed in both hemispheres. For example, between ~4 and 3.5 ka BP, basin wide drier conditions occurred near the contemporary southern limit of the austral summer ITCZ in the southern Indian Ocean as indicated by proxy records from Zambezi Delta (Schefuβ et al., 2011), Tatos Basin (de Boer et al., 2014), Rodrigues and northwest Australia (Denniston et al., 2013) (Figs. 7 and 8). Additionally, a high resolution record from Sahiya cave (Kathayat et al., 2017), located at the northern limit of the boreal summer ITCZ, also show a synchronously drying trend between 4.0 and 3.5 ka BP (Fig. 9).

Additionally, in parallel with drier condition in the southern limit of the austral summer ITCZ, proxy records from Lake Edward (Russell et al., 2003), Lake Victoria (Berke et al., 2012) and Tangga cave (Wurtzel et al., 2018), which lie near the north limit of the contemporary austral summer ITCZ also exhibit dry conditions. In contrast to the dry condition on both northern and southern limits of the austral summer ITCZ, records within the core location of the austral summer ITCZ, such as Lake Challa (Tierney et al., 2011), Lake Tanganyika (Tierney et al., 2008), Lake Malawi (Konecky et al., 2011) and Makassar Strait (Tierney et al., 2012), show either slightly wetter or virtually unchanged hydroclimatic condition (Figs. 7 and 8). Based on these observations, we suggest that the ITCZ contraction in terms of both north-south meridional shift as well as in its overall width may have played an important role in producing the hydroclimatic changes in our study area. Furthermore, changes in the strength of the SH westerly winds (SHW) (Marx et al., 2011; Saunders et al., 2018) also appear to correlate to the megadrought event observed in the Rodrigues record (Fig. 7), which may have restricted the southern range of the austral summer ITCZ.

5 Author Contributions

H.C., A.S. and H.Y.L designed the research and experiments; H.C., A.S., J.B., Y.F.N. and H.Y.L. completed the fieldwork; H.Y.L., H.C., Y.F.N. and C.S. performed all stable isotope measurements and ^{230}Th dating work. A.S., L.Y. and H.Y.L. did the data analyses. H.C., H.Y.L. and A.S. wrote the manuscript, with the help of all other co-authors.

6 Competing interests

The authors declare no competing financial interests.

7 Acknowledgments

This work was supported by grants from NSFC (41472140, 41731174 and 41561144003); US NSF grant 1702816; and a grant from State Key Laboratory of Loess and Quaternary Geology, Institute of Earth Environment, CAS (SKLLQG1414).

Clim. Past Discuss., https://doi.org/10.5194/cp-2018-100
Manuscript under review for journal Clim. Past
Discussion started: 27 August 2018

Climate of the Past Discussions

8 Data and materials availability

All data needed to evaluate the conclusions in the paper are presented in the paper. Additional data related to this paper may be requested from the authors. The data will be archived at the National Climate Data Center (https://www.ncdc.noaa.gov/data-access/paleoclimatology-data). Correspondence and requests for materials should be addressed to H.C. (cheng021@xjtu.edu.cn).

References:

Adler, R. F., Sapiano, M. R., Huffman, G. J., Wang, J. J., Gu, G., Bolvin, D., Chiu, L., Schneider, U., Becker, A., Nelkin, E., Xie, p., Ferraro, R., Shin, D.: The Global Precipitation Climatology Project (GPCP) Monthly Analysis (New Version 2.3) and a Review of 2017 Global Precipitation, Atmosphere, 9, 138, 2018.

Arz, H.W., Lamy, F., and Pätzold, J.: A pronounced dry event recorded around 4.2 ka in brine sediments from the northern Red Sea, Quaternary Research, 66, 432–441, 2006.

Baker, A., Ito, E., Smart, P. L., and McEwan, R. F.: Elevated and variable values of 13C in speleothems in a British cave system, Chemical Geology, 136, 263-270, 1997.

Bar-Matthews, M., Ayalon, A., Kaufman, A., and Wasserburg, G. J.: The Eastern Mediterranean paleoclimate as a reflection of regional events: Soreq cave, Israel, Earth and Planetary Science Letters, 166, 85-95, 1999.

Barron, J. A., and Anderson, L.: Enhanced Late Holocene ENSO/PDO expression along the margins of the eastern North Pacific, Quaternary International, 235(1-2), 3-12, 2011.

Berke, M. A., Johnson, T. C., Werne, J. P., Grice, K., Schouten, S., and Damsté, J. S. S.: Molecular records of climate variability and vegetation response since the Late Pleistocene in the Lake Victoria basin, East Africa, Quaternary Science Reviews, 55, 59-74, 2012.

Boer, E.J.D., Hooghiemstra, H., Florens, F.B.V., Baider, C., Engels, S., Dakos, V., Blaauw, M., and Bennett, K.D.: Rapid succession of plant associations on the small ocean island of Mauritius at the onset of the Holocene, Quaternary Science Reviews, 68, 114-125, 2013.

Boer, E.J.D., Tjallingii, R., Vélez, M.I., Rijsdijk, K.F., Vlug, A., Reichart, G.J., Prendergast, A.L., Louw, P.G.B.D., Florens, F.B.V., and Baider, C.: Climate variability in the SW Indian Ocean from an 8000-yr long multi-proxy record in the Mauritian lowlands shows a middle to late Holocene shift from negative IOD-state to ENSO-state, Quaternary Science Reviews, 86, 175-189, 2014.

Boer, E.J.D., Velez, M.I., Rijsdijk, K.F., Louw, P.G.D., Vernimmen, T.J., Visser, P.M., Tjallingii, R., and Hooghiemstra, H.: A deadly cocktail: How a drought around 4200 cal. yr BP caused mass mortality events at the infamous 'dodo swamp' in Mauritius, Holocene, 25, 2015.

Breitenbach, S.F.M., Rehfeld, K., Goswami, B., Baldini, J.U.L., Ridley, H.E., Kennett, D.J., Prufer, K.M., Aquino, V.V., Asmerom, Y., Polyak, V.J., Cheng, H., Kurths, J., and Marwan, N.: COnstructing Proxy Records from Age models (COPRA), Climate of the past, 8, 1765–1779, 2012.

Brook, G. A., Burney, D. A., and Cowart, J. B.: Desert paleoenvironmental data from cave speleothems with examples from the Chihuahuan, Somali-Chalbi, and Kalahari deserts, Palaeogeography, Palaeoclimatology, Palaeoecology, 76, 311-329, 1990.

Cheng, H., Edwards, R., Hoff, J., Gallup, C., Richards, D., and Asmerom, Y.: The half-lives of uranium-234 and thorium-230, Chemical Geology, 169, 17–33, 2000.

Cheng, H., Edwards, R.L., Shen, C.-C., Polyak, V.J., Asmerom, Y., Woodhead, J., Hellstrom, J., Wang, Y., Kong, X., and Spötl, C.: Improvements in ^{230}Th dating, ^{230}Th and ^{234}U half-life values, and U–Th isotopic measurements by multi-collector inductively coupled plasma mass spectrometry, Earth and Planetary Science Letters, 371, 82–91, 2013.

Conroy, J. L., Overpeck, J. T., Cole, J. E., Shanahan, T. M., and Steinitz-Kannan, M.: Holocene changes in eastern tropical Pacific climate inferred from a Galápagos lake sediment record, Quaternary Science Reviews, 27, 1166-1180, 2008.

Edwards, R.L., Chen, J., and Wasserburg, G.: ^{238}U- ^{234}U- ^{230Th}- ^{232}Th systematics and the precise measurement of time over the past 500,000 years, Earth and Planetary Science Letters, 81, 175–192, 1987.

Dansgaard, W.: Stable isotopes in precipitation, Tellus, 16, 436–468, 1964.

Denniston, R.F., Wyrwoll, K.H., Polyak, V.J., Brown, J.R., Asmerom, Y., Jr, A.D.W., Lapointe, Z., Ellerbroek, R., Barthelmes, M., and Cleary, D.: A Stalagmite record of Holocene Indonesian–Australian summer monsoon variability from the Australian tropics, Quaternary Science Reviews, 78, 155-168, 2013.

Denniston, R. F., Ummenhofer, C. C., Wanamaker, A. D., Lachniet, M. S., Villarini, G., Asmerom, Y., Polyak, V. J., Passaro, K. J., Cugley, J., Woods, D., and Humphreys, W. F.: Expansion and contraction of the Indo-Pacific tropical rain belt over the last three millennia, Scientific Reports, 6, 34485. 2016.

Donders, T. H., Wagner-Cremer, F., and Visscher, H.: Integration of proxy data and model scenarios for the mid-Holocene onset of modern ENSO variability, Quaternary Science Reviews, 27, 571-579, 2008.

Dorale, J. A., González, L. A., Reagan, M. K., Pickett, D. A., Murrell, M. T., and Baker, R. G.: A high-resolution record of Holocene climate change in speleothem calcite from Cold Water Cave, northeast Iowa, Science, 258, 1626-1630, 1992.

Dorale, J. A., and Liu, Z.: Limitations of Hendy test criteria in judging the paleoclimatic suitability of speleothems and the need for replication, Journal of Cave and Karst Studies, 71, 73-80, 2009.

Draxler, R. R., and Hess, G. D.: An overview of the HYSPLIT_4 modelling system for trajectories, Australian meteorological magazine, 47, 295-308, 1998.

Finné, M., Holmgren, K., Sundqvist, H. S., Weiberg, E., and Lindblom, M.: Climate in the eastern Mediterranean, and adjacent regions, during the past 6000 years–A review, Journal of Archaeological Science, 38, 3153-3173, 2011.

Freitas, A. C. V., Aímola, L., Ambrizzi, T., and de Oliveira, C. P.: Extreme Intertropical Convergence Zone shifts over Southern Maritime Continent, Atmospheric Science Letters, 18, 2-10, 2017.

Fohlmeister, J.: A statistical approach to construct composite climate records of dated archives, Quaternary Geochronology, 14, 48–56, 2012.

Genty, D., Blamart, D., Ouahdi, R., Gilmour, M., Baker, A., Jouzel, J., and Van-Exter, S.: Precise dating of Dansgaard–Oeschger climate oscillations in western Europe from stalagmite data, Nature, 421, 833, 2003.

Griffiths, M.L., Drysdale, R.N., Gagan, M.K., Zhao, J.X., Ayliffe, L.K., Hellstrom, J.C., Hantoro, W.S., Frisia, S., Feng, Y.X., and Cartwright, I.: Increasing Australian-Indonesian monsoon rainfall linked to early Holocene sea-level rise, Nature Geoscience, 2, 636-639, 2009.

Griffiths, M. L., Kimbrough, A. K., Gagan, M. K., Drysdale, R. N., Cole, J. E., Johnson, K. R., Zhao, J. X., Cook, B. I., Hellstrom, J. C., and Hantoro, W. S.: Western Pacific hydroclimate linked to global climate variability over the past two millennia, Nature communications, 7, 11719, 2016.

Jaffey, A. H., Flynn, K. F., Glendenin, L. E., Bentley, W. T., and Essling, A. M.: Precision measurement of half-lives and specific activities of ^{235}U and ^{238}U, Physical Review C, 4, 1889, 1971.

Kalnay, E., Kanamitsu, M., Kistler, R., Collins, W., Deaven, D., Gandin, L., Iredell, M., Saha, S., White, G., Woollen, J., Zhu, Y., Chelliah, M., Ebisuzaki, W., Higgins, W., Janowiak, J., Mo, K.C., Ropelewski, C., Wang, J., Leetmaa, A., Reynolds, R., Jenne, R. and Joseph, D.: The NCEP/NCAR 40-year reanalysis project, Bulletin of the American meteorological Society, 77, 437-472, 1996.

Kathayat, G., Cheng, H., Sinha, A., Yi, L., Li, X., Zhang, H., Li, H., Ning, Y., and Edwards, R.L.: The Indian monsoon variability and civilization changes in the Indian subcontinent, Science advances, 3, e1701296, 2017.

Konecky, B. L., Russell, J. M., Johnson, T. C., Brown, E. T., Berke, M. A., Werne, J. P., and Huang, Y.: Atmospheric circulation patterns during late Pleistocene climate changes at Lake Malawi, Africa, Earth and Planetary Science Letters, 312, 318-326, 2011.

Lashkari, H., Mohammadi, Z., and Keikhosravi, G.: Annual Fluctuations and Displacements of Inter Tropical Convergence Zone (ITCZ) within the Range of Atlantic Ocean-India, Open Journal of Ecology, 7, 12, 2017.

Marchant, R., and Hooghiemstra, H.: Rapid environmental change in African and South American tropics around 4000 years before present: a review, Earth-Science Reviews, 66, 217-260, 2004.

Marx, S. K., Kamber, B. S., McGowan, H. A., and Denholm, J.: Holocene dust deposition rates in Australia's Murray-Darling Basin record the interplay between aridity and the position of the mid-latitude westerlies, Quaternary Science Reviews, 30, 3290-3305, 2011.

Mayewski, P.A., Rohling, E.J., Stager, J.C., Karlén, W., Maasch, K.A., Meeker, L.D., Meyerson, E.A., Gasse, F., Van Kreveld, S., Holmgren, K., Lee-Thorp, K., Rosqvist, G., Rack, F., Staubwasser, M., Schneider, R.R., and Steig, E.J.: Holocene Climate Variability, Quaternary Research, 62, 243-255, 2004.

Middleton, G. J., and David A. B.: Rodrigues–An Indian Ocean Island calcarenite: its history, study and management, Coastal Karst Landforms, Springer, Dordrecht, 261-276, 2013.

Migowski, C., Stein, M., Prasad, S., Negendank, J. F., and Agnon, A.: Holocene climate variability and cultural evolution in the Near East from the Dead Sea sedimentary record, Quaternary Research, 66, 421-31, 2006.

Monnin, E., Indermühle, A., Dällenbach, A., Flückiger, J., Stauffer, B., Stocker, T. F. Raynaud, D., and Barnola, J. M.: Atmospheric CO2 concentrations over the last glacial termination, Science, 291, 112-114, 2001.

Morioka, Y., Takaya, K., Behera, S. K., and Masumoto, Y.: Local SST impacts on the summertime Mascarene high variability, Journal of Climate, 28, 678-694, 2015.

Railsback, L.B., Liang, F., Brook, G.A., Voarintsoa, N.R.G., Sletten, H.R., Marais, E., Hardt, B., Cheng, H., and Edwards, R.L.: The timing, two-pulsed nature, and variable climatic expression of the 4.2 ka event: A review and new high-resolution stalagmite data from Namibia, Quaternary Science Reviews, 186, 78-90, 2018.

Rienecker, M.M., Suarez, M.J., Gelaro, R., Todling, R., Bacmeister, J., Liu, E., Bosilovich,M.G., Schubert, S.D., Takacs, L., Kim, G.-K., Bloom, S., Chen, J., Collins, D., Conaty, A., da Silva, A., Gu, W., Joiner, J., Koster, R.D., Lucchesi, R., Molod, A., Owens, T., Pawson, S., Pegion, P., Redder, C.R., Reichle, R., Robertson, F.R., Ruddick, A.G., Sienkiewicz, M., and Woollen, J.: MERRA: NASA's Modern-Era Retrospective Analysis for Research and Applications. Journal of Climate, 24, 3624-3648, 2011.

Rijsdijk, K.F., Hume, J.P., Bunnik, F., Florens, F.B.V., Baider, C., Shapiro, B., Plicht, J.V.D., Janoo, A., Griffiths, O., and Ostende, L.W.V.D.H.: Mid-Holocene vertebrate bone Concentration-Lagerstätte on oceanic island Mauritius provides a window into the ecosystem of the dodo (Raphus cucullatus), Quaternary Science Reviews, 28, 14-24, 2009.

Rijsdijk, K.F., Zinke, J., Louw, D.P.G.B., Hume, J.P., Plicht, V.D.H., Hooghiemstra, H., Meijer, H.J.M., Vonhof, H.B., Porch, N., and Florens, F.B.V.: Mid-Holocene (4200 yr BP) mass mortalities in Mauritius (Mascarenes): insular vertebrates resilient to climatic extremes but vulnerable to human impact, Holocene, 21, 1179-1194, 2011.

Russell, J.M., Johnson, T.C., and Talbot, M.R.: A 725 yr cycle in the climate of central Africa during the late Holocene, Geology, 31, 677-680, 2003.

Russell, J. M., and Johnson, T. C.: Late Holocene climate change in the North Atlantic and equatorial Africa: Millennial-scale ITCZ migration, Geophysical Research Letters, 32, L17705, 2005.

Saunders, K.M., Roberts, S.J., Perren, B., Butz, C., Sime, L., Davies, S., Nieuwenhuyze, W. V., Grosjean, M., and Hodgson, D. A.: Holocene dynamics of the Southern Hemisphere westerly winds and possible links to CO2 outgassing, Nature Geoscience. 2018

Schefuß, E., Schouten, S. and Schneider, R.R.: Climatic controls on central African hydrology during the past 20,000 years, Nature, 437, 1003, 2005.

Schefuß, E., Kuhlmann, H., Mollenhauer, G., Prange, M., and Pätzold, J.: Forcing of wet phases in southeast Africa over the past 17,000 years, Nature, 480, 509, 2011.

Scroxton, N., Burns, S. J., McGee, D., Hardt, B., Godfrey, L. R., Ranivoharimanana, L., and Faina, P.: Hemispherically in-phase precipitation variability over the last 1700 years in a Madagascar speleothem record, Quaternary Science Reviews, 164, 25-36, 2017.

Senapathi, D., Underwood, F., Black, E., Nicoll, M. A., and Norris, K. Evidence for long-term regional changes in precipitation on the East Coast Mountains in Mauritius, International Journal of Climatology, 30, 1164-1177, 2010.

Spötl, C., and Vennemann, T. W.: Continuous-flow isotope ratio mass spectrometric analysis of carbonate minerals, Rapid communications in mass spectrometry, 17, 1004-1006, 2003.

Spötl, C.: Long-term performance of the Gasbench isotope ratio mass spectrometry system for the stable isotope analysis of carbonate microsamples, Rapid Communications in Mass Spectrometry, 25, 1683-1685, 2011.

Stanley, J.-D., Krom, M.D., Cliff, R.A., and Woodward, J.C.: Short contribution: Nile flow failure at the end of the Old Kingdom, Egypt: strontium isotopic and petrologic evidence, Geoarchaeology, 18, 395-402, 2003.

Staubwasser, M., Sirocko, F., Grootes, P., and Segl, M.: Climate change at the 4.2 ka BP termination of the Indus valley civilization and Holocene south Asian monsoon variability, Geophysical Research Letters, 30, 2003.

Tierney, J.E., Russell, J.M., Huang, Y., Damsté, J.S.S., Hopmans, E.C., and Cohen, A.S.: Northern Hemisphere Controls on Tropical Southeast African Climate during the Past 60,000 Years, Science, 322, 252-255, 2008.

Tierney, J.E., Russell, J.M., Damsté, J.S.S., Huang, Y., and Verschuren, D.: Late Quaternary behavior of the East African monsoon and the importance of the Congo Air Boundary, Quaternary Science Reviews, 30, 798-807, 2011.

Tierney, J.E., Oppo, D. W., LeGrande, A. N., Huang, Y., Rosenthal, Y., and Linsley, B. K.: The influence of Indian Ocean atmospheric circulation on Warm Pool hydroclimate during the Holocene epoch, Journal of Geophysical Research: Atmospheres, 117. 2012.

Verschuren, D., Damsté, J. S. S., Moernaut, J., Kristen, I., Blaauw, M., Fagot, M., Haug, G. H., and CHALLAXEA project members.: Half-precessional dynamics of monsoon rainfall near the East African Equator, Nature, 462, 637, 2009.

Walker, M. J., Berkelhammer, M., Björck, S., Cwynar, L. C., Fisher, D. A., Long, A. J., Lowe, J.J., Newnham, R.M., and Weiss, H.: Formal subdivision of the Holocene Series/Epoch: a Discussion Paper by a Working Group of INTIMATE (Integration of ice-core, marine and terrestrial records) and the Subcommission on Quaternary Stratigraphy (International Commission on Stratigraphy), Journal of Quaternary Science, 27, 649-659, 2012.

Wanner, H., Beer, J., Bütikofer, J., Crowley, T.J., Cubasch, U., Flükiger, J., Goosse, H., Grosjean, M., Joos, F., Kaplan, J.O., Küttel, M., Müller, S.A., Prentice, I.C., Solomina, O., Stocker, T.F., Tarasov, P., Wagner, M., and Widmann, M.: Mid- to Late Holocene climate change: an overview, Quaternary Science Reviews, 27, 1791-1828, 2008.

Weiss, H., Courty, M.-A., Wetterstrom, W., Guichard, F., Senior, L., Meadow, R., and Curnow, A.: The genesis and collapse of third millennium north Mesopotamian civilization, Science, 261, 995–1004, 1993.

Weiss, H.: Global megadrought, societal collapse and resilience at 4.2-3.9 ka BP across the Mediterranean and west Asia, PAGES, 24, 62–63, 2016.

Wurtzel, J.B., Abram, N.J., Lewis, S.C., Bajo, P., Hellstrom, J.C., Troitzsch, U., and Heslop, D.: Tropical Indo-Pacific hydroclimate response to North Atlantic forcing during the last deglaciation as recorded by a speleothem from Sumatra, Indonesia, Earth and Planetary Science Letters, 492, 264-278, 2018.

Yan, H., Wei, W., Soon, W., An, Z., Zhou, W., Liu, Z., Wang, Y., and Carter, R. M.: Dynamics of the intertropical convergence zone over the western Pacific during the Little Ice Age, Nature Geoscience, 8, 315, 2015.

Yoshimura, K., Kanamitsu, M., Noone, D., and Oki, T.: Historical isotope simulation using reanalysis atmospheric data, Journal of Geophysical Research: Atmospheres, 113, 2008.

Zielhofer, C., Suchodoletz, H.V., Fletcher, W.J., Schneider, B., Dietze, E., Schlegel, M., Schepanski, K., Weninger, B., Mischke, S., and Mikdad, A.: Millennial-scale fluctuations in Saharan dust supply across the decline of the African Humid Period, Quaternary Science Reviews, 171, 119-135, 2017.

Zinke, J., Reuning, L., Pfeiffer, M., Wassenburg, J.A., Hardman, E., Jhangeerkhan, R., Davies, G.R., Ng, C.K.C., and Kroon, D.: A sea surface temperature reconstruction for the southern Indian Ocean trade wind belt from corals in Rodrigues Island (19° S, 63° E), Biogeosciences, 13, 5827-5847, 2016.

Clim. Past Discuss., https://doi.org/10.5194/cp-2018-100
Manuscript under review for journal Clim. Past
Discussion started: 27 August 2018

Figures:

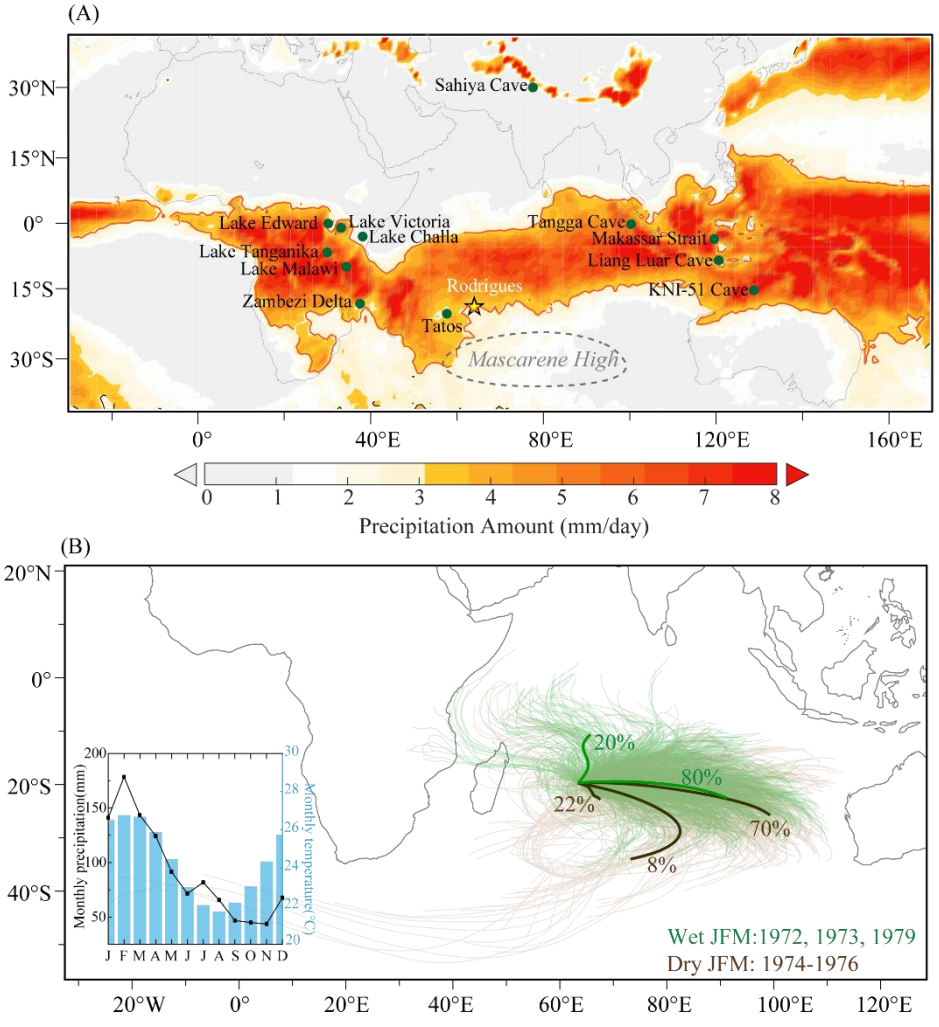

Figure 1. Proxy locations and climatology. (A) The mean January to March (JFM) precipitation from the Tropical Rainfall Measuring Mission (TRMM) (https://trmm.gsfc.nasa.gov/) averaged over the period from 1997 to 2014. Shaded area bounded by solid red lines (3 mm day^{-1} isohyet) depict the mean position of the ITCZ. The dashed line shows the mean position of JFM 850 hPa geopotential height marking the location of the Mascarene High. Locations of Rodrigues Island (yellow star, this study) and other proxy sites (green dots) discussed in the text are also shown. **(B)** 4x daily low-level (~850 hpa) JFM air parcel back (120 hours) trajectory composites for anomalously wet (green) and dry (brown) years. Trajectories were computed using NOAA HYSPLIT model (Draxler and Hess, 1998) using NCEP/NCAR Reanalysis data (Kalnay et al., 1996). Bold lines indicate main cluster tracks associated with trajectories for wetter (green) and drier (brown) years. Inset shows mean monthly rainfall and temperature at Rodrigues averaged over the period from 1951 to 2015.

Clim. Past Discuss., https://doi.org/10.5194/cp-2018-100
Manuscript under review for journal Clim. Past
Discussion started: 27 August 2018

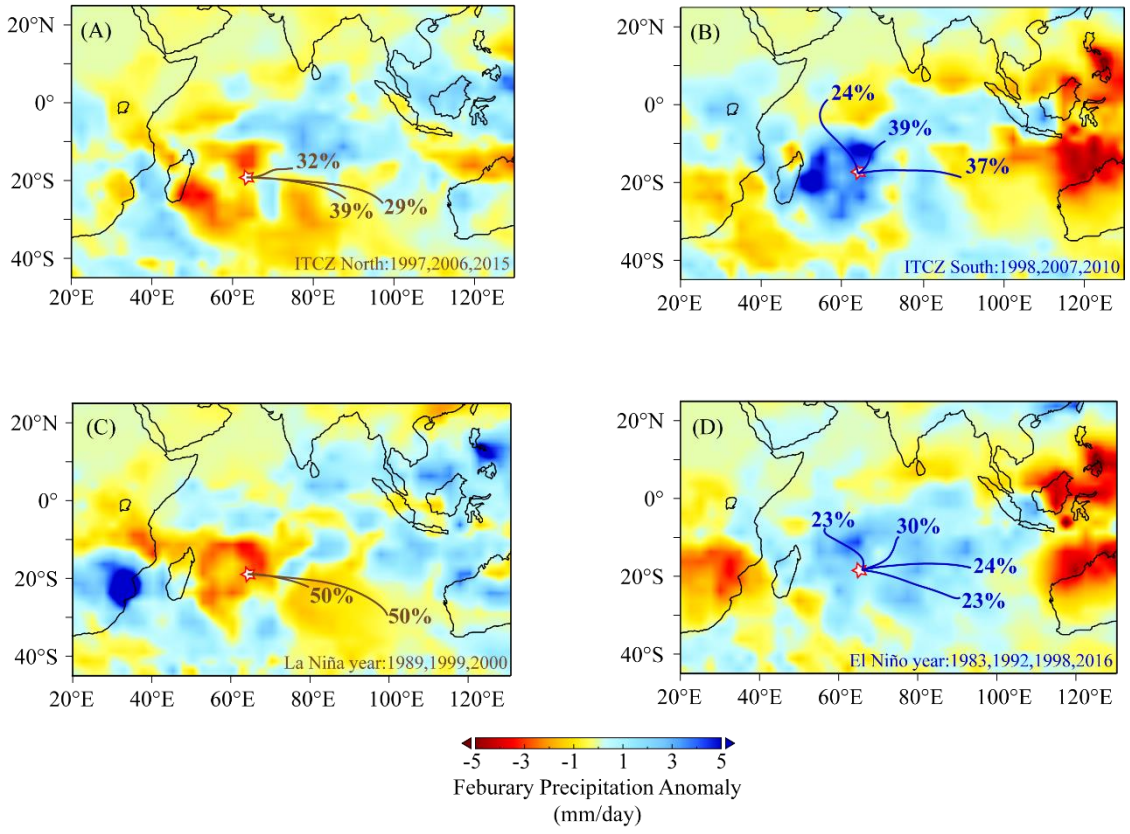

Figure 2. The ITCZ and ENSO dynamics. (A and B) The spatial composite maps of precipitation anomalies for February (anomalies calculated with respect to the period 1981-2010) for the years marked by anomalous northward (A, 1997, 2006, 2015) and southward (B, 1998, 2007, 2010) location of the southern boundary of the ITCZ (Lashkari et al., 2017; Freitas et al., 2017). The maps are overlaid by backward (120 hours) low level air parcel trajectory clusters and their relative contributions. **(C and D)** Same as in **A** and **B** but for the La Niña (C, 1989, 199, 2000) and El Niño (D, 1983, 1992, 1998, 2016) years. Precipitation data is from GPCP (Adler et al., 2018).

Clim. Past Discuss., https://doi.org/10.5194/cp-2018-100
Manuscript under review for journal Clim. Past
Discussion started: 27 August 2018

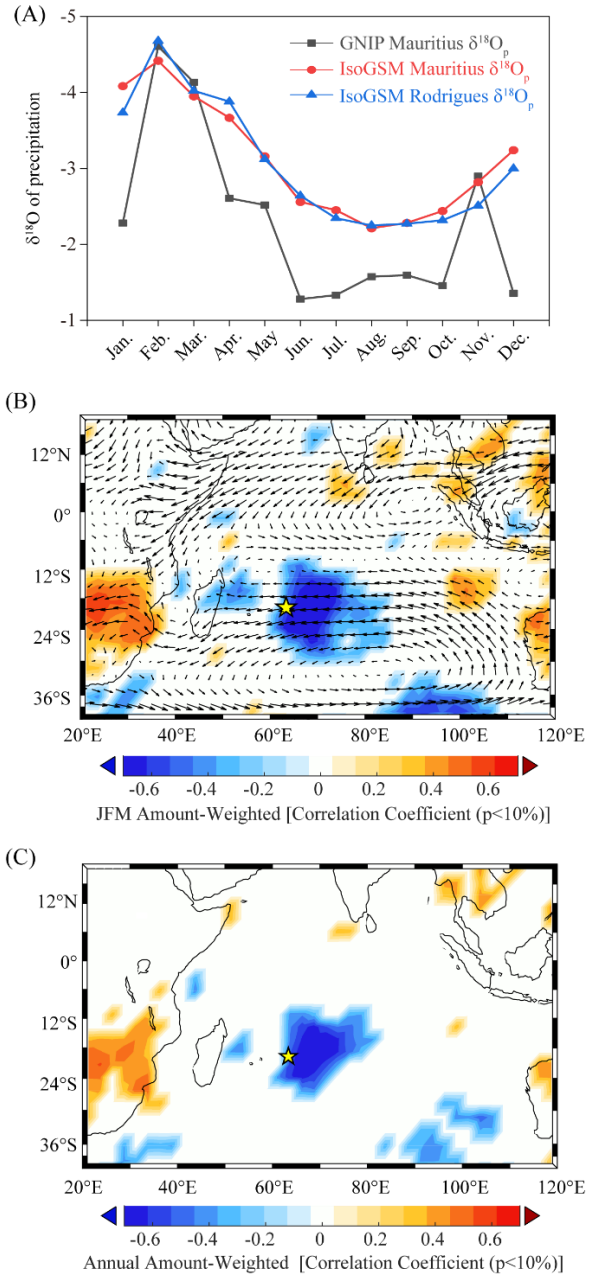

Figure 3. Model and observational data of $\delta^{18}O$ in precipitation in the study area. **(A)** Monthly means of simulated $\delta^{18}O_p$ from Mauritius (red) and Rodrigues (blue) from IsoGSM (Yoshimura et al., 2008). Also shown is monthly means of $\delta^{18}O_p$ from six GNIP stations in Mauritius (black) covering the periods from 1992-1995 and 2009-2014. **(B and C)** The spatial correlation maps for JFM **(B)** and annual **(C)** amount-weighted IsoGSM $\delta^{18}O_p$ from the nearest grid point to Rodrigues and the GPCP precipitation (GPCP v2.3) (Adler et al., 2018) for the period 1979 to 2016.

Clim. Past Discuss., https://doi.org/10.5194/cp-2018-100
Manuscript under review for journal Clim. Past
Discussion started: 27 August 2018

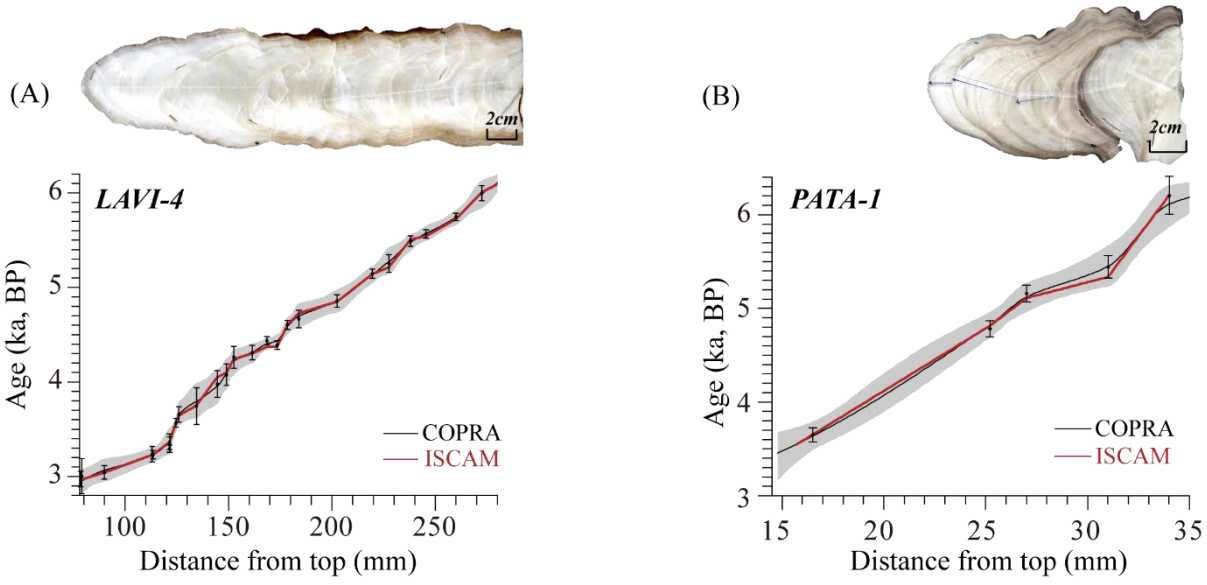

Figure 4. Age models of LAVI-4 and PATA-1 records. (A) LAVI-4 age models and age uncertainties using COPRA (Breitenbach et al., 2012) (black) and ISCAM (Fohlmeister, 2012) (red) modeling methods. The gray band depicts the 95% confidence interval from COPRA. Error bars on ^{230}Th dates represent 2σ analytical errors. (**B**) Same as in **(A)** but for sample PATA-1.

Clim. Past Discuss., https://doi.org/10.5194/cp-2018-100
Manuscript under review for journal Clim. Past
Discussion started: 27 August 2018

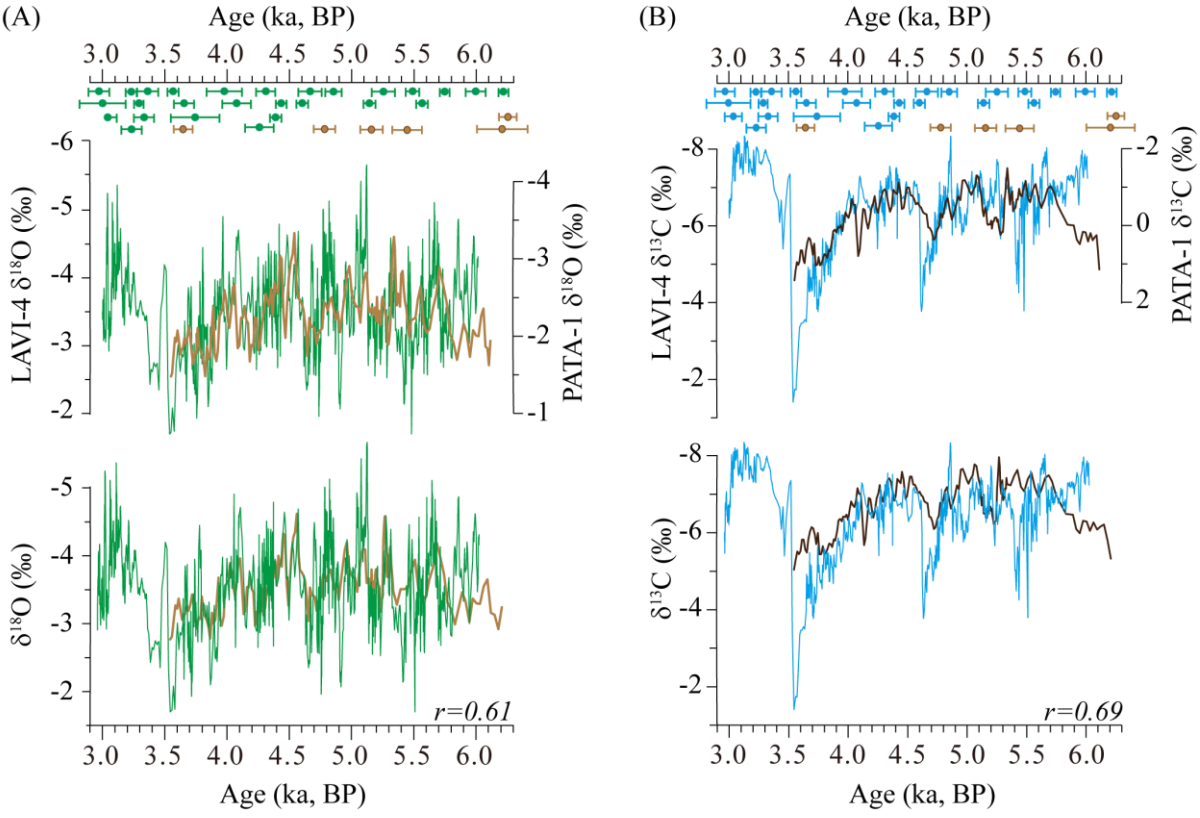

Figure 5. $\delta^{18}O$ and $\delta^{13}C$ records of LAVI-4 and PATA-1. (A) The $\delta^{18}O$ profiles of LAVI-4 (green) and PATA-1 (brown) on their independent COPRA (Breitenbach et al., 2012) age models (top) and ISCAM (Fohlmeister, 2012) derived age models (bottom). The correlation coefficient (*r*) between LAVI-4 and PATA-1 is *0.61*. The PATA 1 $\delta^{18}O$ values were adjusted by ~1.5 ‰ to match with the LAVI-4. **(B)** Same as in **(A)** but for the $\delta^{13}C$ profiles of LAVI-4 and PATA-1. The PATA-1 $\delta^{13}C$ values were adjusted by ~6.7 ‰ to match with the LAVI-4 values.

Clim. Past Discuss., https://doi.org/10.5194/cp-2018-100
Manuscript under review for journal Clim. Past
Discussion started: 27 August 2018

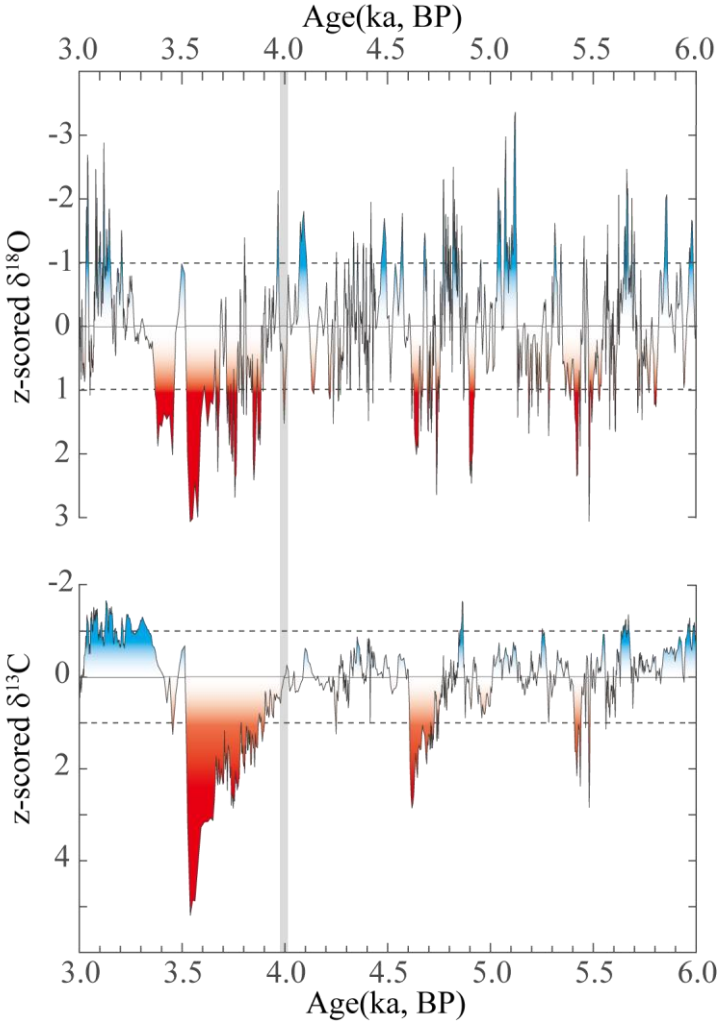

Figure 6. The inferred hydroclimatic variability at Rodrigues from 6 to 3 ka BP. The LAVI-4 $\delta^{18}O$ and $\delta^{13}C$ record shown as z-score transformed. Inferred drought (z-score > 1) and pluvial (z-score < -1) are shaded (increasing saturation index indicates increasing intensity). Dash lines indicate the 1 standard deviation. Grey bar at ~4 ka BP mark the beginning of multi-centennial period of drier condition.

Clim. Past Discuss., https://doi.org/10.5194/cp-2018-100
Manuscript under review for journal Clim. Past
Discussion started: 27 August 2018

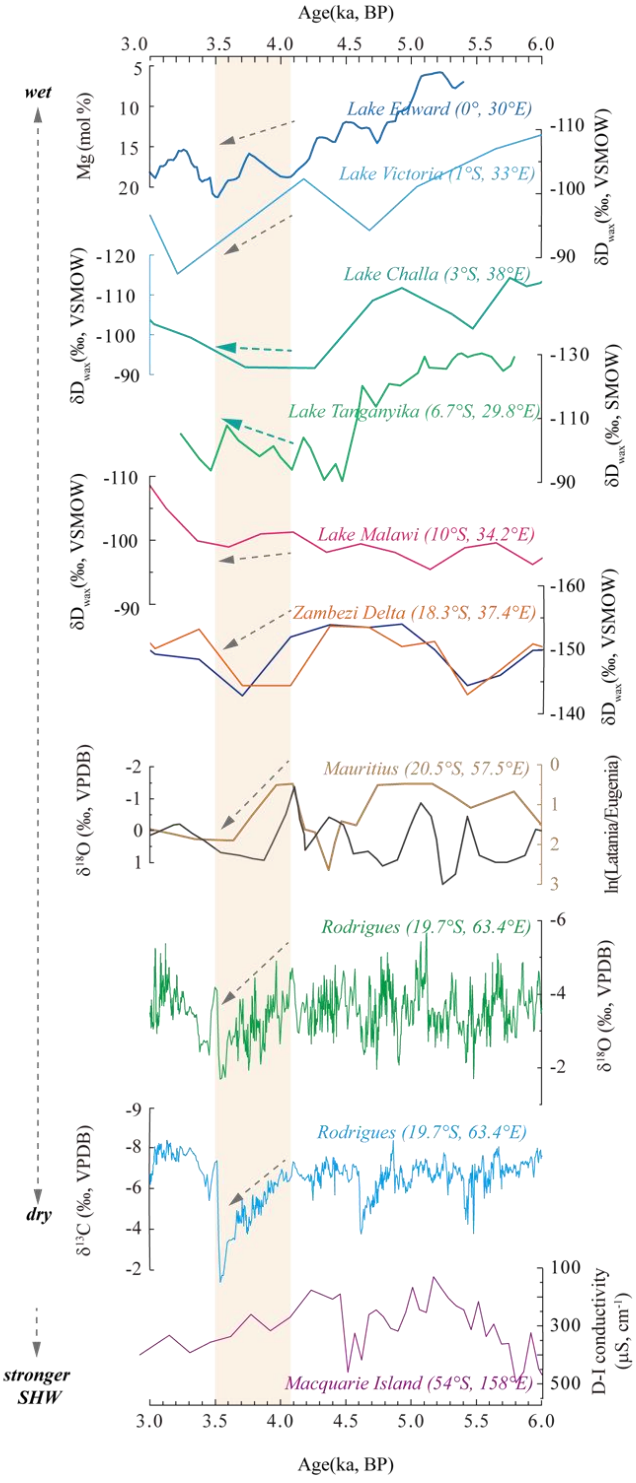

Figure 7. Comparison of LAVI-4 with climate proxy records from East Africa and Macquarie Island. From top to bottom, Mg concentration of sedimentary endogenic calcite from Lake Edward

Clim. Past Discuss., https://doi.org/10.5194/cp-2018-100
Manuscript under review for journal Clim. Past
Discussion started: 27 August 2018

(Russell et al., 2003); the $\delta D_{leaf\ wax}$ records from Lake Victoria (Berke et al., 2012); Lake Challa (Tierney et al., 2011); Lake Tanganyika (Tierney et al., 2008); Lake Malawi (Konecky et al., 2011); the δD of the n-C_{29} alkane (dark blue) and the n-C_{31} alkane (orange) from Zambezi delta (Schefuβ et al., 2011); the $\delta^{18}O$ record (black) and ln (Latania/Eugenia) records (brown) from Tatos basin, Mauritius (de Boer et al., 2014); the LAVI-4 $\delta^{18}O$ and $\delta^{13}C$ record from La Vierge cave (this study); and the D-I conductivity from Lake Emerald, Macquarie Island (Saunders et al., 2018). Shaded vertical bar marks the duration from ~ 4.1 to 3.5 ka BP. Grey and green dashed arrows mark the drying and wet trend inferred from East Africa lake records, respectively. All y axes (except for the Macquarie island profile) are inverted to show drier conditions down.

Clim. Past Discuss., https://doi.org/10.5194/cp-2018-100
Manuscript under review for journal Clim. Past
Discussion started: 27 August 2018

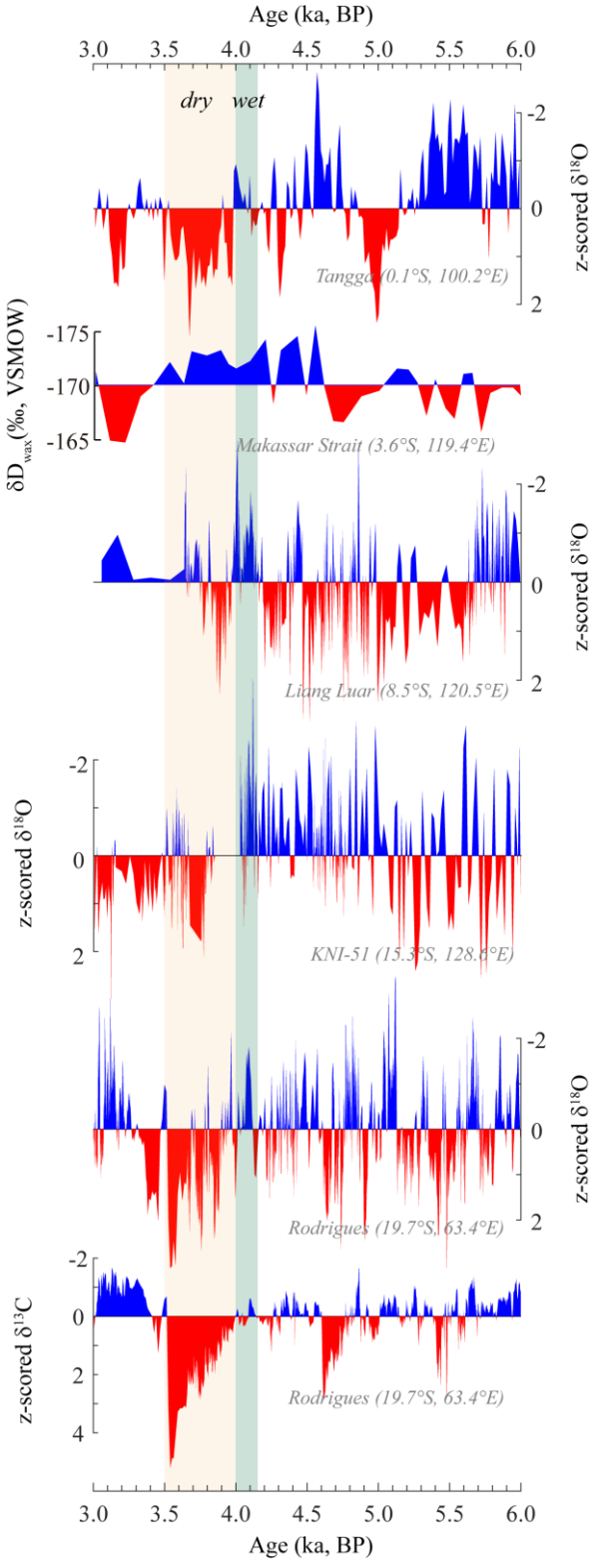

Clim. Past Discuss., https://doi.org/10.5194/cp-2018-100
Manuscript under review for journal Clim. Past
Discussion started: 27 August 2018

Climate of the Past Discussions
Open Access
EGU

Figure 8. Comparison of LAVI 4 with climate proxy records from the eastern Indian Ocean. From top to bottom, z-score transformed speleothem $\delta^{18}O$ record from Tangga cave, Sumatra, Indonesia (Wurtzel et al., 2018); the $\delta D_{leaf\ wax}$ record from marine sediment core BJ8-03-70GGC in the Makassar Strait (Tierney et al., 2012); z-score transformed speleothem $\delta^{18}O$ records from Ling Luar western Flores, Indonesia (Griffiths et al., 2009); KNI-51 cave, Kimberley, northwestern Australia (Denniston et al., 2013); and LAVI-4 $\delta^{18}O$ and $\delta^{13}C$ records from La Vierge cave (this study). Shaded vertical bars mark periods of drier and wetter conditions.

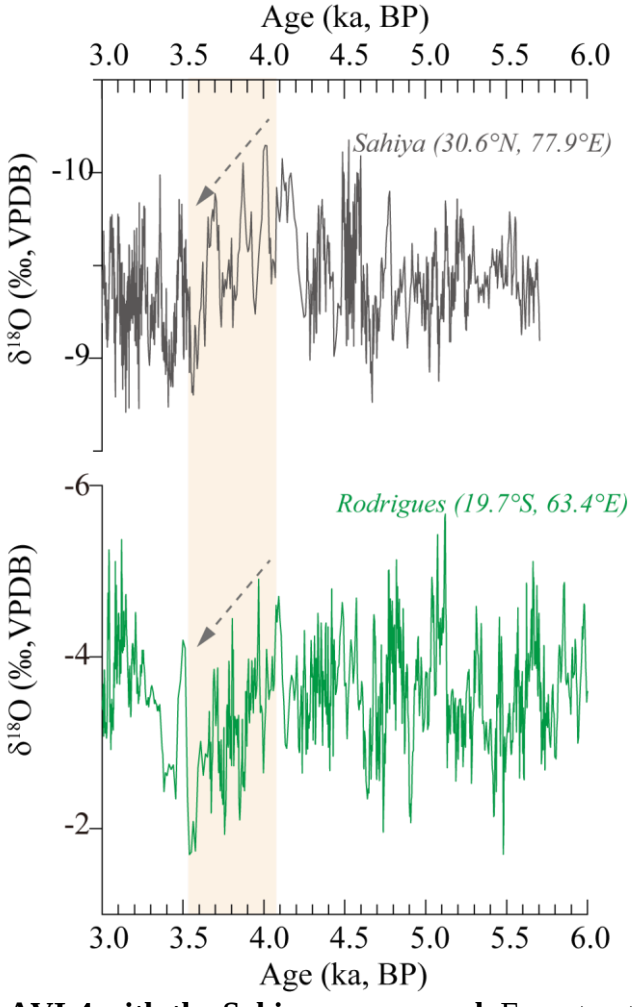

Figure 9. Comparison of LAVI-4 with the Sahiya cave record. From top to bottom, speleothem $\delta^{18}O$ record from Sahiya cave, North India (Kathayat et al., 2017). Shaded bar marks the duration from ~ 4 to 3.5 ka BP. Grey dashed arrow line mark the drying trend inferred from both records.